The Influence of Mg on Creep Properties and Fracture Behaviors of Mar-M247 Superalloy under 1255 K/200 MPa

H.Y. BOR, C.G. CHAO, and C.Y. MA

The effects of Mg microadditions on the high-temperature/low stress (1255 K/200 MPa) creep properties and fracture behavior of a Mar-M247 superalloy were investigated in this study. The results of quantitative statistical analyses showed that when Mg microadditions up to 50 ppm were made, the MC carbides located at grain boundaries (designated GB MC) were significantly refined and spheroidized and the number of MC carbides decreased. In addition, the $M_{23}C_6$ carbides present on GBs dramatically increased with increasing Mg contents up to 50 ppm, and the creep resistance was enhanced under the test condition of 1255 K/200 MPa. However, the creep performance of a Mar-M247 superalloy containing 80 ppm Mg deteriorated due to the formation of an extremely large amount of MC carbide and a decrease in the number of $M_{23}C_6$ carbides at GBs. The cracks mainly initiated and propagated along GBs in both the Mg-free and Mg-containing Mar-M247 superalloys under 1255 K/200 MPa, and the finial rupture was caused by intergranular fracture. Under the present creep condition, the optimal Mg microaddition to a Mar-M247 superalloy should be 30 to 50 ppm.

I. INTRODUCTION

THE Mar-M247 superalloy was first introduced in 1972 by Martin Metals, a Division of Martin Marietta (Baltimore, MD). The merits of Mar-M247 include good castability, as well as excellent creep and oxidation resistance at elevated temperatures.[1–4] Over the past 2 decades, this alloy has been widely applied in fabricating advanced turbine blades and rotating parts in the aerospace industry. However, based on previous studies,[5,6] Mar-M247 has been found to have a low ductility under creep conditions of moderate temperatures and high stresses. This problem is reported to be related to the presence of elongated or scriptlike MC carbides[7,8,9] which act as crack-initiation sites and as propagation paths.[6,9,10] In order to minimize this detrimental effect, the refinement of the coarse MC carbides through microalloying is thought to be a desirable solution.

It has been reported[11–22] that small amounts of Mg added to several wrought superalloys enhance the toughness, hot workability, creep life, and ductility of these alloys. In recent investigations,[9,23–25] it has been shown that the microaddition of Mg in directionally solidified and conventional cast superalloys can also improve the solidification behavior and structure. The Mg segregates to the carbide/matrix interface, leading to a refinement of the primary MC carbide and inhibiting the scriptlike carbide formation.[9,23,26] According to our previous study,[9] the creep life and rupture elongation of a Mar-M247 superalloy containing 30 to 80 ppm Mg could be effectively improved under a moderate temperature/high stress condition (1033 K/724 MPa). In addition, the tensile elongation obtained at 1172 K reached 14 pct, which is 3 times greater than the engine material specification (EMS-55447) requirement.[5] Thus, the problem of low elongation at moderate temperature appears to be successfully resolved. According to EMS-55447,[5] the creep properties of a Mar-M247 superalloy must satisfy requirements under two test conditions, *i.e.*, at a moderate temperature/high stress (1033 K/724 MPa) and a high temperature/low stress (1255 K/200 MPa). However, the influence of microadditions of Mg on the high temperature/low stress properties and fracture mechanism in Mar-M247 superalloy is still equivocal.

In this study, the effects of Mg microadditions on the creep behavior of a Mar-M247 superalloy at 1255 K/200 MPa were investigated in detail. The objectives of this investigation were to study the characteristic changes of grain boundary (GB) carbide caused by Mg microadditions to the Mar-M247 superalloy and to determine the suitable contents of Mg to add to a Mar-M247 superalloy to promote the creep properties.

II. EXPERIMENTAL

The Mar-M247 superalloy employed in this study was prepared by vacuum induction melting followed by remelting it in a vacuum induction furnace and then precision casting into standard test bars. The pouring and mold temperatures were the same as in our previous study.[9] Various Mg contents ranging from 0 to 80 ppm were added to the Mar-M247 superalloy during remelting. After casting, the Mg content in each heat was analyzed by glow discharge mass spectrometry (GDMS), and the chemistry of the major elements was detected by X-ray fluorescence (XRF). The compositions of each heat used in the present investigation are given in Table I. Among them, the Mg content of alloy 1 (8 ppm) originated from the raw or crucible materials during primary melting. All test bars were solution treated at 1458 K for 2 hours and aged at 1144 K for 20 hours in a vacuum furnace.

The microstructure was characterized by scanning electron microscopy (SEM) and high resolution transmission election microscopy (HRTEM). The GB carbide characteristics, including particle size, aspect ratio, linear density, and fraction, were measured and identified from at least ten

H.Y. BOR and C.Y. MA, Associate Scientists, are with the Materials and Electro-optics Research Division, Chung-Shan Institute of Science and Technology, Taiwan 325, Republic of China. C.G. CHAO, Professor, is with the Institute of Materials Science and Engineering, National Chiao-Tung University, Hsin-Chu, Taiwan 300, Republic of China.

Manuscript received June 3, 1998.

Table I. Chemical Composition (Weight Percent) of Mar-M247 Superalloys Analyzed by XRF for Major Elements and GDMS for Mg

Heat Number	Co	Cr	Mo	W	Ta	Ti	Al	Hf	Zr	C	Mg	Ni
EMS-55447	9.0 to 11.0	8.0 to 8.8	0.5 to 0.8	9.5 to 10.5	2.8 to 3.3	0.9 to 1.2	5.3 to 5.7	1.2 to 1.6	0.03 to 0.08	0.13 to 0.17	—	bal
1*	10.1	8.32	0.69	9.91	3.16	1.00	5.56	1.51	0.05	0.15	0.0008	bal
2	10.1	8.20	0.71	9.86	3.17	1.04	5.69	1.37	0.04	0.15	0.002	bal
3	10.2	8.24	0.73	9.95	3.11	1.02	5.54	1.31	0.04	0.15	0.003	bal
4	10.2	8.21	0.71	9.86	3.09	1.00	5.57	1.31	0.04	0.15	0.005	bal
5	10.1	8.14	0.72	9.74	3.00	0.97	5.47	1.29	0.04	0.15	0.008	bal

*The Mg content (8 ppm) of heat 1 originated from raw or crucible materials.

different GBs possessing more than 400 carbides. The quantitative statistical analyses adopted an artificial calculation way to differentiate the MC carbide (2 to 10 μm) and $M_{23}C_6$ carbide (0.2 to 0.8 μm) at the GB. In accordance with EMS-55447, high-temperature creep tests were conducted at 1255 K/200 MPa using the same SATEC M3 creep testers as in our previous results[9] where creep tests were performed at 1033 K/724 MPa. The gage size of the test bars was 6.3 mm in diameter and 26 mm in length. The fractography was examined in a JEOL*-6400 SEM equipped with energy dispersive spectroscopy (EDS) for microanalysis.

*JEOL is a trademark of Japan Electron Optics Ltd., Tokyo.

III. RESULTS

A. *Microstructure and Characteristics of GB Carbides*

The microstructure of the Mar-M247 superalloy after heat treatment is shown in Figure 1. Two types of carbide were observed to precipitate at the GB, fine and discrete $Cr_{23}C_6$ as well as coarse and elongated MC carbides, while the main carbides that existed in the matrix were Ta- or Hf-enriched MC carbides.[9] According to previous image-analysis results,[9] the optimal microaddition of Mg could refine the coarse MC carbides in the matrix and inhibit the precipitation of scriptlike carbides in a Mar-M247 superalloy. The grain size (2 to 3 mm) obtained under the present condition was independent of Mg addition and solidified into a radial pattern.

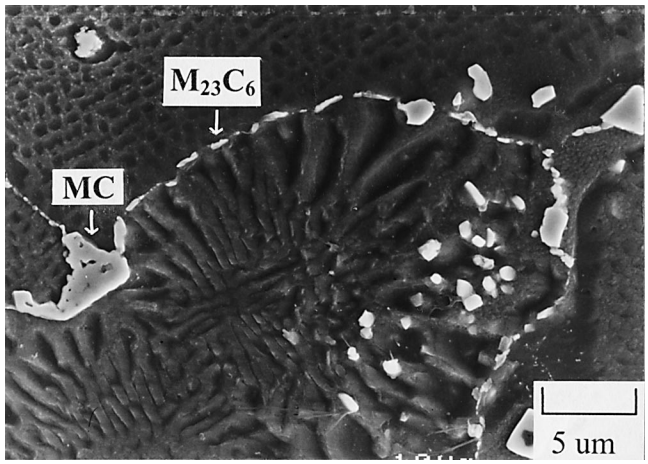

Fig. 1—Microstructure of a Mg-free Mar-M247 superalloy after heat treatment.

Figure 2 illustrates the characteristic changes in the carbides located at the GB due to the microaddition of various Mg contents. For a Mg-free Mar-M247 superalloy, a number of small $M_{23}C_6$ ($Cr_{23}C_6$) particle carbides precipitated at the GB during the heat treatment with their size ranging from 0.2 to 0.8 μm (Figures 2(a) and (b)). Another type of carbide distributed along the GB was a Ta-, Hf-, or W-enriched MC carbide (Figure 2(c)) with a size ranging from 2 to 10 μm. These carbides were also identified and determined by HRTEM, as shown in Figures 3 and 4. Figure 5 shows a microstructure in the vicinity of a GB in a 30 ppm Mg alloy. The major precipitate at the GB was still the Cr-rich $M_{23}C_6$ carbide with the blocky MC carbide being occasionally present along the GB. When 80 ppm Mg was added, a number of MC carbides precipitated at the GB while the $M_{23}C_6$ carbide density decreased (Figure 6). Thus, the microaddition of 80 ppm Mg refined the MC carbides both within the grain interior and at the GB, while the number of MC carbides present at the GB increased.

Figure 7 shows the quantitative statistical results concerning GB carbide characteristics in a Mar-M247 superalloy with various Mg contents. Figure 7(a) demonstrates that the MC carbide particle size was reduced to 3.1 μm from a size of 5.2 μm in the Mg-free alloy; *i.e*, the coarse GBs MC carbides were refined due to the microaddition of Mg. Figure 7(b) shows that as the Mg content increased, the aspect ratio of GBs MC carbides was lower, which means that spheroidization of the GBs MC carbides was achieved from the Mg addition. Figure 7(c) shows the linear density of MC carbides along the GB. It is obvious that the number of GBs MC carbides decreased as the amount of Mg was raised to 50 ppm. However, the number of MC carbide particles in the Mar-M247 containing 80 ppm Mg was 2 times greater than that of the Mar-M247 superalloy with 50 ppm Mg. On the other hand, the number of $M_{23}C_6$ carbides in the 80 ppm Mg alloy greatly decreased, as shown in Figure 7(d). The fraction of the GB covered by MC carbides was extremely high (42.0 pct) for the alloy containing 80 ppm Mg, and this value was approximately twice that of the MC carbide in alloys containing 30 or 50 ppm Mg. It is evident that the Mar-M247 superalloy with 80 ppm Mg had an extremely large amount of MC carbides precipitated at the GB. The result led to a decrease in the amount of $M_{23}C_6$ carbide, although the refinement and spheroidization of the MC carbides were achieved.

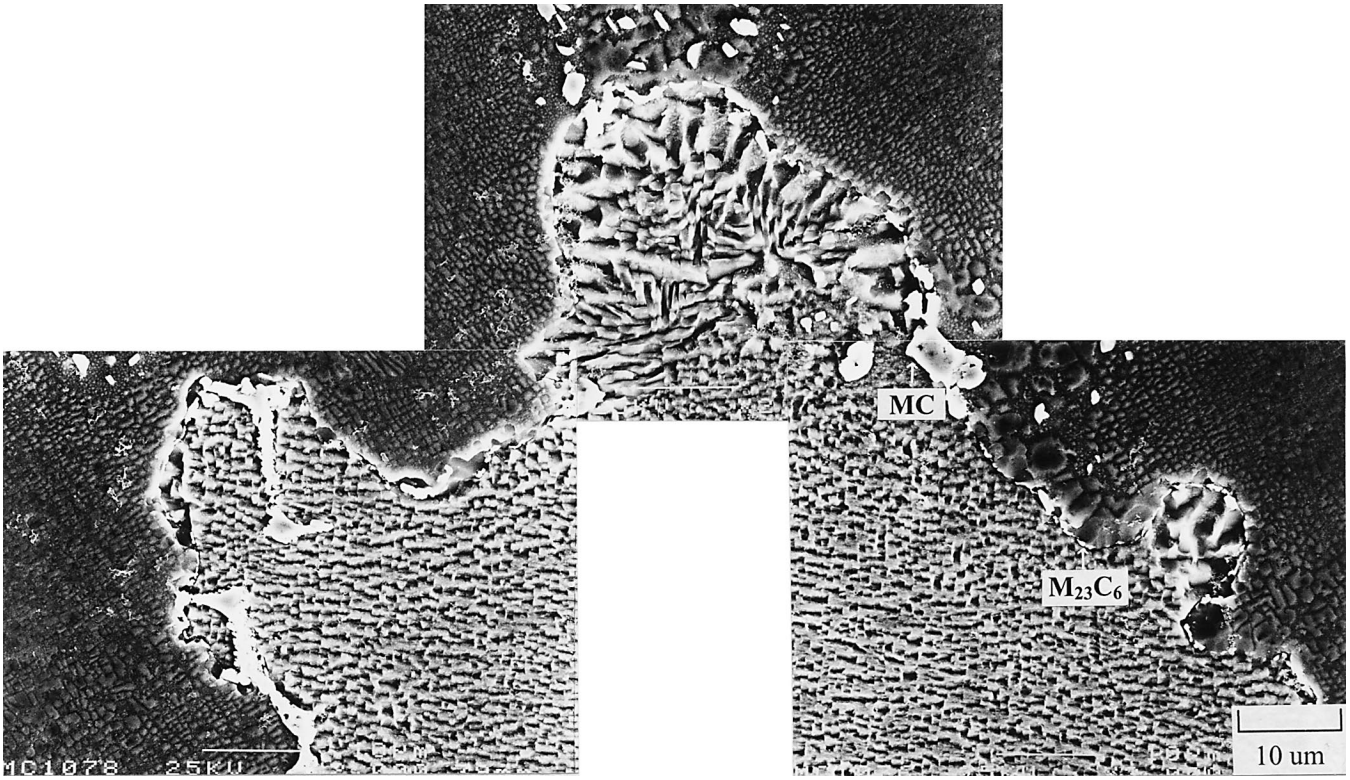

(*a*)

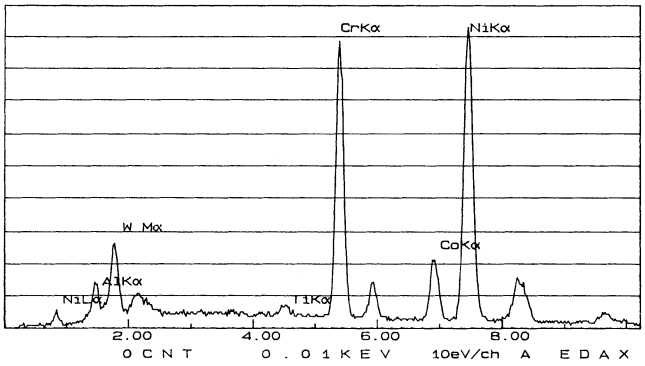

(*b*)

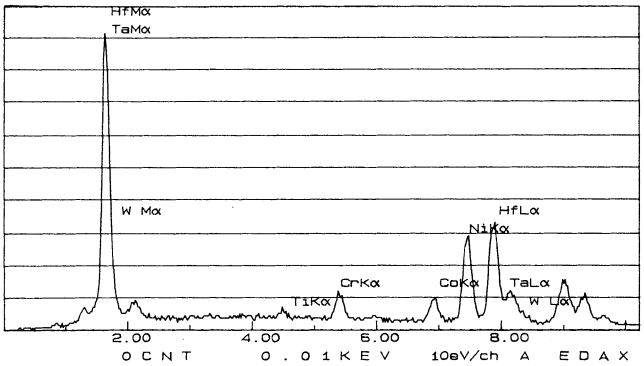

(*c*)

Fig. 2—(*a*) The morphology of carbides at a GB in the Mg-free Mar-M247 superalloy, (*b*) the EDS analysis results of a $M_{23}C_6$ carbide at the GB, and (*c*) the EDS analysis results of a MC carbide at the GB.

B. *Creep Tests*

According to EMS-55447, the rupture life of a Mar-M247 superalloy creep tested under conditions of 1255 K/200 MPa must be greater than 25 hours and the elongation should not be lower than 4 pct. As shown in Table II, the rupture elongation and life increased with Mg content up to 50 ppm. In particular, when the Mg content was 50 ppm, the rupture elongation and life reached 5.7 pct and 145 hours, respectively. Also, it is obvious that the period of steady-state creep was around 60 to 70 hours in the Mar-M247 superalloy containing 30 to 50 ppm Mg (Table II), demonstrating a superior creep behavior compared to the other alloys tested.

However, when 80 ppm of Mg was added, the creep life and elongation of the Mar-M247 decreased and the steady-state creep rate increased. In addition, the period of steady-state creep also sharply declined. These observations demonstrate that the creep behavior of Mar-M247 deteriorated by the continued addition of Mg. Table III lists the time required to achieved strains of 1 and 2 pct in the Mar-M247 superalloy at various Mg contents. The creep-strain life was prolonged with increasing Mg contents up to 50 ppm. However, the alloy containing 80 ppm Mg possessed a significantly shorter life, showing the detrimental effect of Mg overadditions.

C. *Fractographic Observation*

In order to investigate the effect of Mg microadditions on the fracture mode, observations were made from the longitudinal section adjacent to the fracture. For the Mg-free specimen, a carbide film of 1 to 2 μm in thickness was clearly found at the fracture position, as shown in Figure 8(a). Further examination of the interior, approximately 100 μm from the fracture surface, showed that two grains had already separated during creep and fracture occurred along

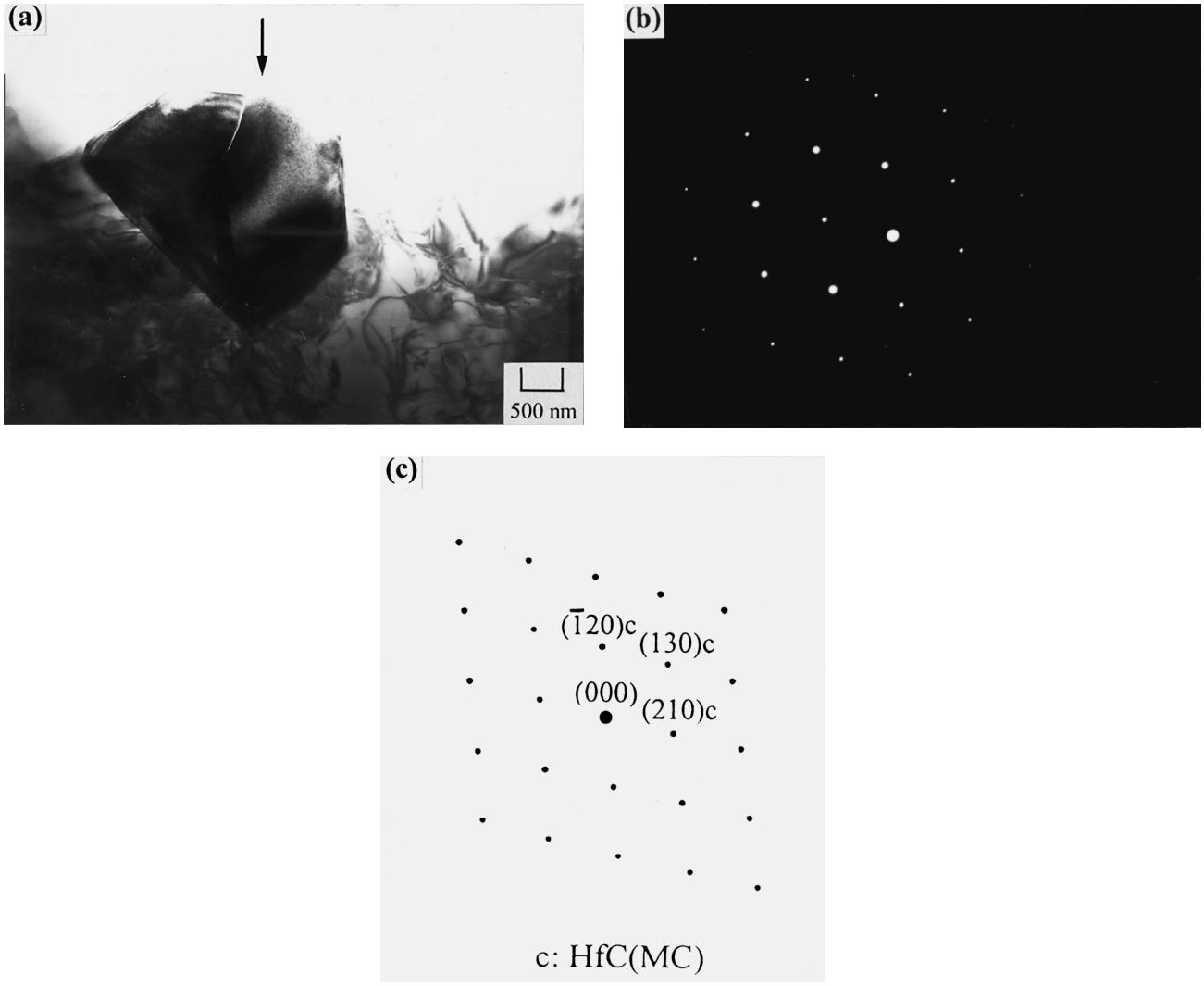

Fig. 3—HRTEM images of a HfC (MC type) carbide: (*a*) bright field, (*b*) selected area diffraction pattern (SADP), and (*c*) interpretation of SADP.

the GBs, as shown in Figure 8(b), indicating a typical intergranular fracture. This result is different from our previous study in which specimens were tested under 1033 K/724 MPa, and a mixture mode of transgranular and intergranular fracture was found to be dominant.[9] Similar observations were made in the alloys containing 30 to 50 ppm Mg, and rupture took place along the $Cr_{23}C_6$ located at GBs (Figure 9). For a specimen containing 80 ppm Mg, an examination of the microstructure of the fracture region illustrated that crack initiation and propagation also occurred along GBs. However, the fracture was now controlled by the presence of Hf-, Ta-, and W-riched MC carbides, as shown in Figure 10. Hence, under the condition of high temperature and low stress, the fracture mode in the Mar-M247 superalloy was now intergranular with the type of carbide-controlling rupture determined by the amount of Mg.

IV. DISCUSSION

A. *Influence of Mg on GB Carbide Characteristics*

The microstructural observations and quantitative analyses have proved that Mg has a great influence on the size, number, morphology, distribution, and quantity of the carbide phases at GBs. According to previous results,[9,23,26] Mg is a surface-active element and has a high propensity for segregating to MC carbide/matrix interface, causing a Mg-enriched layer to develop and surround the carbides during solidification. Once formed, the Mg-enriched layer might influence the transport of carbon and carbide forming elements, such as Hf, Ta, or W. It results in the isotropic growth of carbides during solidification and eventually leads to the refinement and spheroidization of MC carbides both at the GB and within the grain interior in Mar-M247 superalloy.

According to the present results, an optimal Mg addition (30 and 50 ppm) inhibited the precipitation of coarse MC carbide and caused the formation of a number of $M_{23}C_6$ carbides at the GB. Conversely, an addition of 80 ppm Mg gave rise to a number of MC carbides precipitated at the GB, although these MC carbides were observed to be refined and spheroidized. In addition, due to the formation of the MC carbides at the GB, the number of GB $M_{23}C_6$ carbides sharply declined in the 80 ppm Mg Mar-M247 superalloy. The reasons responsible for this change remain unknown. It might be related to a reduction of MC carbides in matrix

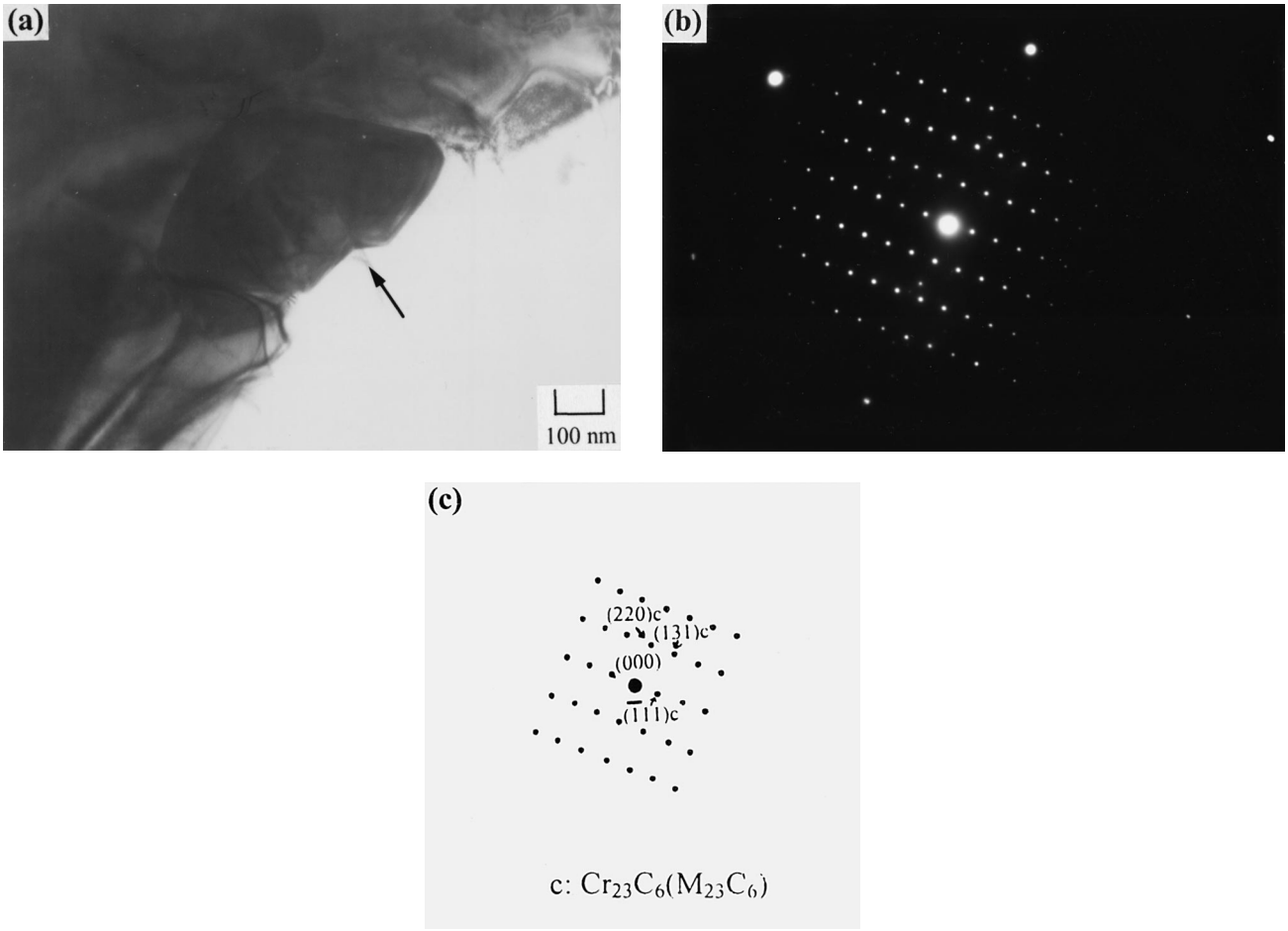

Fig. 4—HRTEM images of a $Cr_{23}C_6$ ($M_{23}C_6$ type) carbide: (*a*) bright field, (*b*) SADP, and (*c*) interpretation of SADP.

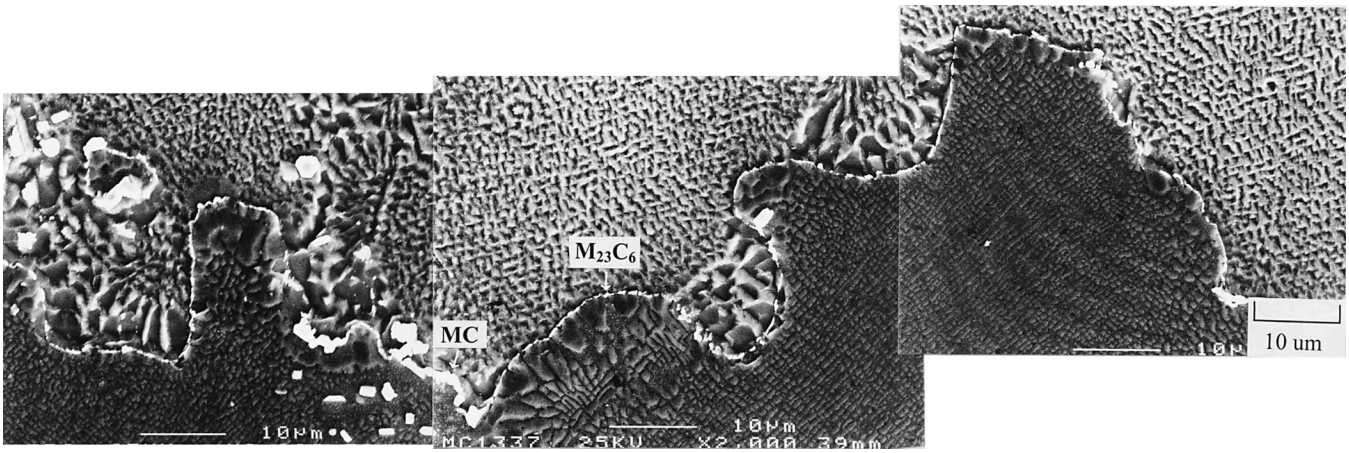

Fig. 5—The morphology of carbides at a GB in the 30 ppm Mg Mar-M247 superalloy.

and inhibition of scriptlike carbide formation when Mg is overadded.[9] In other words, the overaddition of Mg could cause the precipitation of MC carbide more easily at GBs as a result of an increase in the supersaturation of carbon. Thus, more studies should be performed to examine this phenomenon.

B. *Creep Behavior and Fracture Mechanism*

According to the observation of fracture surface from longitudinal section, the GBs become the sites at which rupture initiates under 1255 K/200 MPa. The morphology and distribution of carbides at GBs are the major factors in determining creep behavior. Generally, a large number of fine $M_{23}C_6$ carbides are beneficial for GB strengthening and for inhibiting GB migration. Sims[27] and Gresham[28] have emphasized that improved elevated-temperature rupture life can be obtained when the GBs are decorated with discrete $M_{23}C_6$ carbide particles. Conversely, the presence of coarse and a large number of GBs MC carbides have to be minimized. According to the present study, the microaddition of

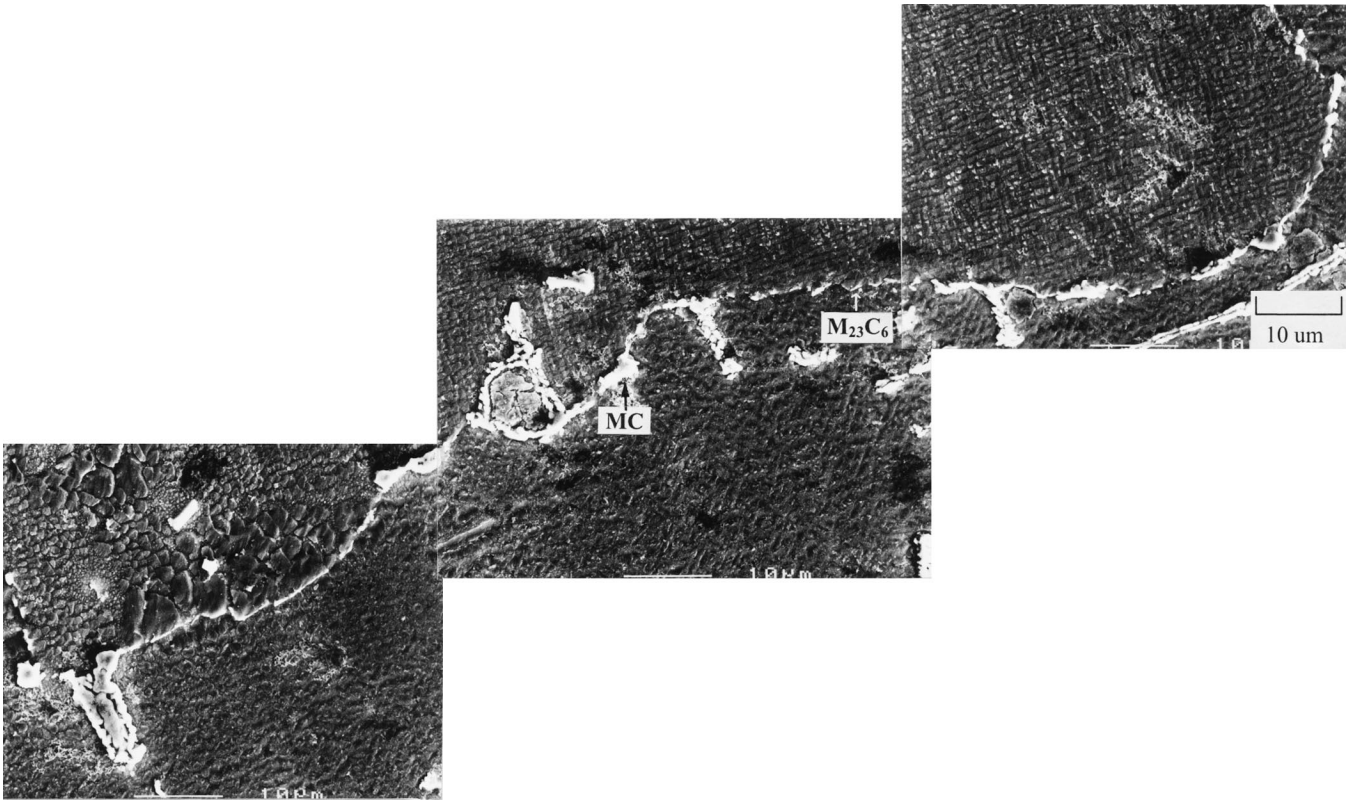

Fig. 6—The morphology of carbides at a GB in the 80 ppm Mg Mar-M247 superalloy.

30 to 50 ppm Mg not only refined and spheroidized the MC carbides but also resulted in a low content of blocky MC carbide at GBs. Moreover, a relatively large amount of small and discrete $M_{23}C_6$ carbides precipitated at the GB in the alloys. On this basis, the rupture life and elongation under the high temperature/low stress creep condition were effectively prolonged. Likewise, the Mar-M247 superalloys with 30 to 50 ppm Mg possessed a longer life at creep strains of 1 and 2 pct as compared with those observed for Mg-free and 80 ppm Mg alloys. Typically, when 80 ppm of Mg was incorporated, an exceptionally high amount of MC carbide precipitated at the GB, resulting in the sharp decrease of $M_{23}C_6$ carbides. It has been reported that coarse GBs MC carbides could weaken the boundaries and enhance intergranular cracking.[7,10] This resulted in a decrease in creep life and ductility at the 1255 K/200 MPa condition as well. Under the condition of our previous article where creep was conducted at 1033 K/724 MPa,[9] however, the elongated and scriptlike MC carbides in the matrix were apparently refined and spheroided in 80 ppm Mg alloy. This led to a change of stress state in front of the carbides. As a result, the creep life and rupture elongation of the Mar-M247 superalloy with 80 ppm Mg could be improved up to 3 to 5 times that of alloy without Mg during the 1033 K/724 MPa creep test.

Hence, strictly controlled Mg contents could have a positive influence on the properties of the alloys while the overaddition of Mg would impair the creep behavior. It is clear from the experimental results that there existed a range of optimum Mg contents, and under or overaddition of Mg resulted in a departure from the best creep properties. In this study, the microaddition of 30 to 50 ppm Mg was necessary to obtain the optimum GB carbide characteristics and excellent creep properties under the high-temperature/low stress(1255 K/200 MPa) creep-test condition.

V. CONCLUSIONS

In summary, the effects of Mg microadditions on the GB carbide characteristics and high-temperature/low stress creep behavior as well as the fracture mechanism in a Mar-M247 superalloy are as follows:

1. The Mg microaddition produced a refinement and spheroidization of MC carbides at GBs. The number of MC carbides at GBs decreased with the Mg content up to 50 ppm. However, when Mar-M247 contained 80 ppm Mg, a number of MC carbides precipitated at the GB, causing a decrease in the number of small $M_{23}C_6$ carbides.
2. Due to the large amount of $M_{23}C_6$ and relatively low number of MC carbides on the GBs, the microaddition of 30 to 50 ppm Mg in a Mar-M247 superalloy could enhance the creep resistance under a 1255 K/200 MPa creep condition. However, the rupture life and elongation in the 80 ppm Mg alloy significantly decreased because of the large amount of MC carbides at the GB.
3. The cracks mainly initiated and propagated along GBs in both the Mg-free and Mg-containing Mar-M247 superalloys at 1255 K/200 MPa. The final rupture was caused by intergranular fracture, and the fracture mode under the present creep condition was mainly controlled by carbide characteristics at the GB.

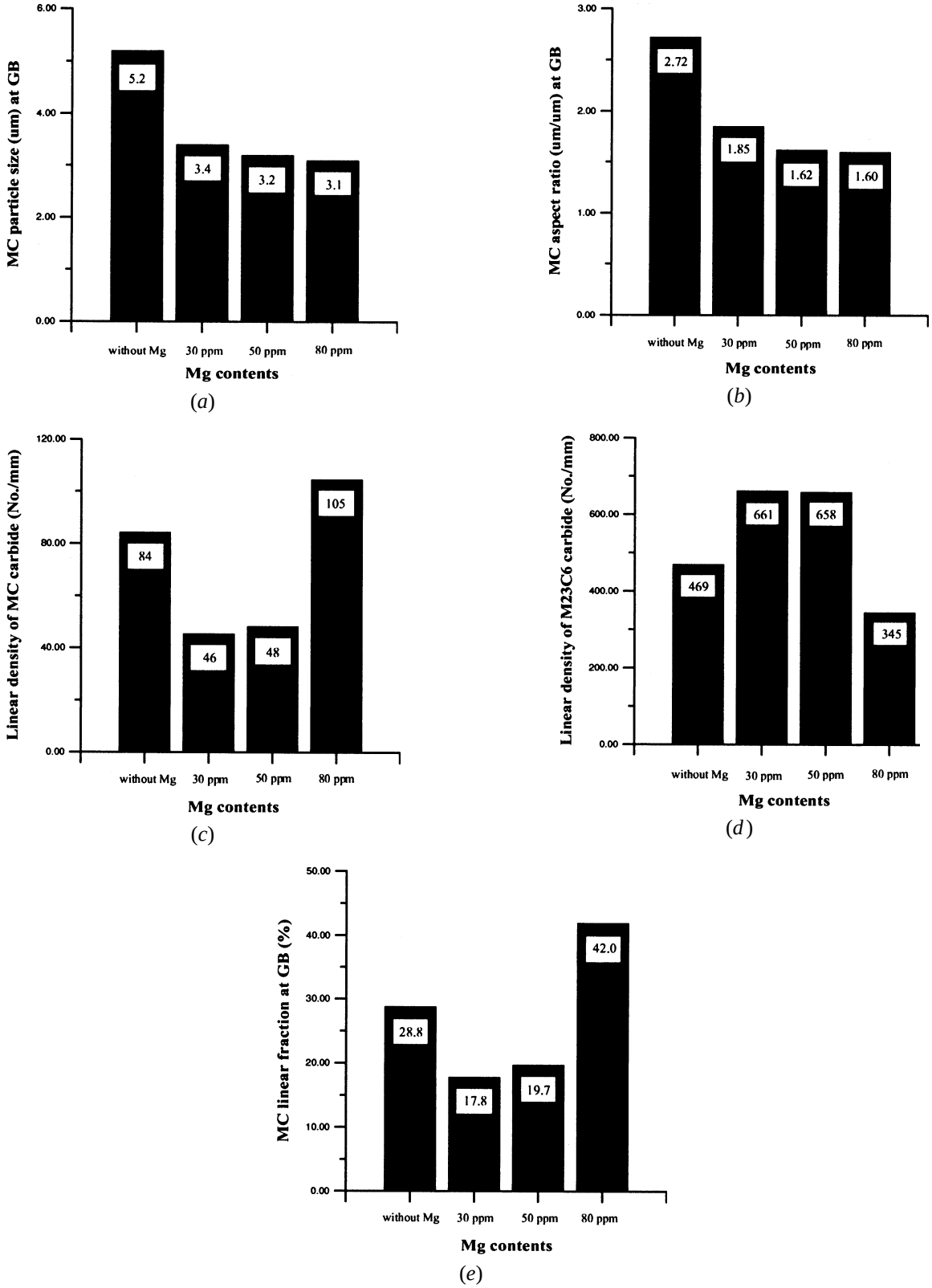

Fig. 7—Quantitative analysis results of GB carbide characteristics in Mar-M247 superalloys with various Mg contents: (*a*) particle size of the MC carbides, (*b*) aspect ratio of the MC carbides, (*c*) linear density of the MC carbides, (*d*) linear density of the $M_{23}C_6$ carbides, and (*e*) MC carbide linear fraction on the GB.

4. The optimal Mg contents for prompting creep behavior should be determined on the basis of the service condition and fracture mode in the Mar-M247 superalloy. Under the present creep condition, the alloys containing 30 to

Table II. Creep Test Results of Mar-M247 under 1255 K/200 MPa

Mg Contents	Creep Life (h)	Elongation (Pct)	Creep Rate (s^{-1})	Period of Steady-State Creep (h)
EMS-55447	>25	>4	—	—
Without Mg	105 to 125	4.3 to 5.2	5.0×10^{-8}	38.9
20 ppm Mg	122 to 146	4.7 to 5.3	4.7×10^{-8}	47.2
30 ppm Mg	136 to 149	4.8 to 5.3	3.4×10^{-8}	62.5
50 ppm Mg	136 to 145	4.6 to 5.7	3.2×10^{-8}	72.2
80 ppm Mg	83 to 116	3.8 to 4.4	4.9×10^{-8}	29.2

Table III. Creep Strain Life of Mar-M247 under 1255 K/200 MPa

Mg Contents	Time to 1 Pct Creep (h)	Time to 2 Pct Creep (h)
EMS 55447	—	—
Without Mg	35.8	78.4
20 ppm Mg	45.2	91.2
30 ppm Mg	50.0	106.0
50 ppm Mg	70.0	113.0
80 ppm Mg	42.5	79.7

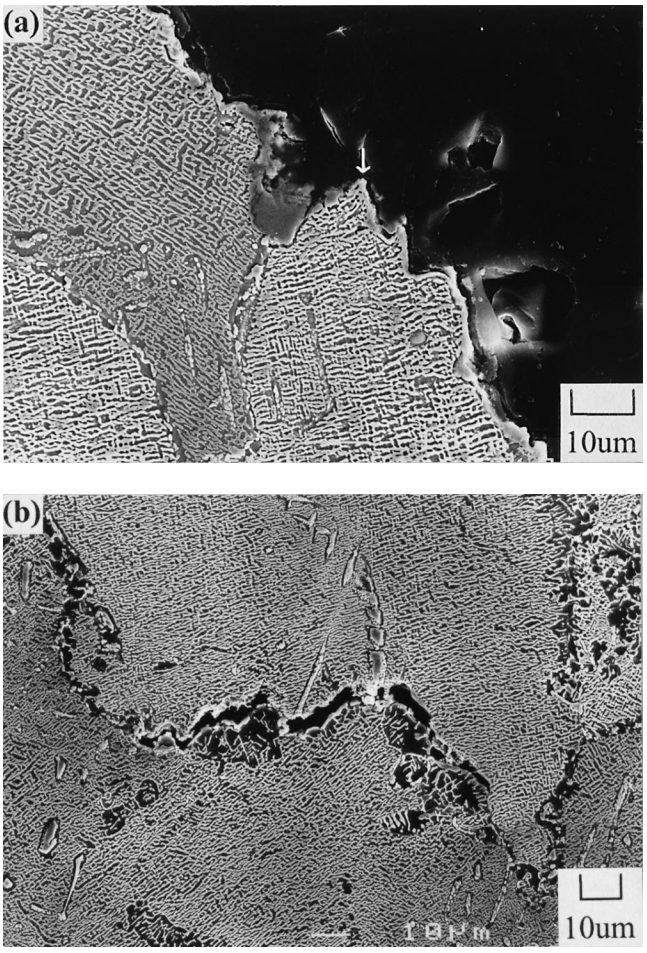

Fig. 8—Longitudinal section of a crept Mar-M247 superalloy without Mg tested under 1255 K/200 MPa: (*a*) at the fracture position and (*b*) 100 μm from the fracture surface.

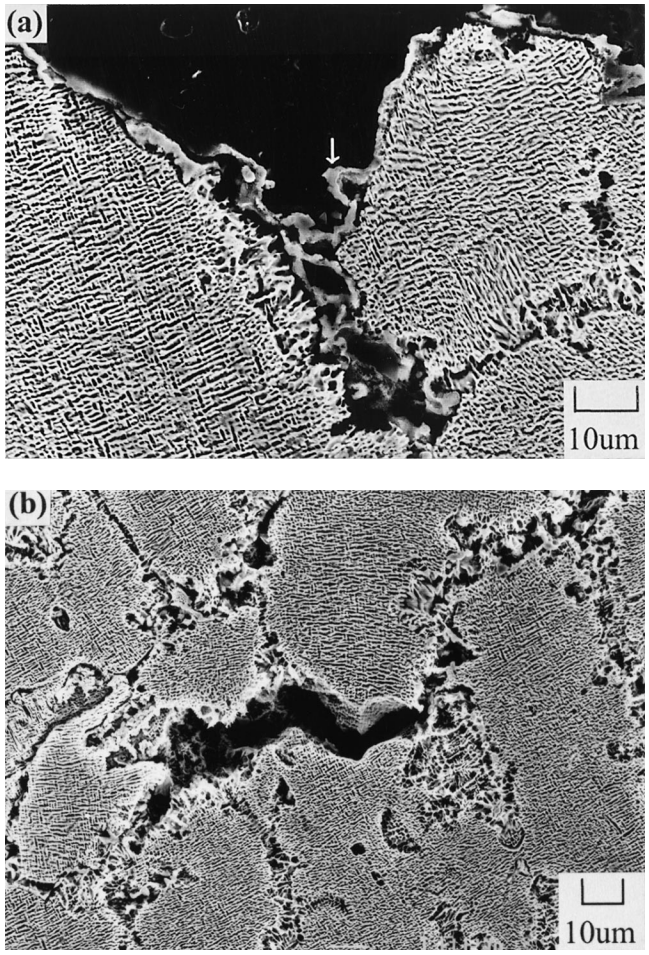

Fig. 9—Longitudinal section of a crept Mar-M247 superalloy with 30 ppm Mg tested under 1255 K/200 MPa: (*a*) at the fracture position and (*b*) 100 μm from the fracture surface.

50 ppm Mg possessed excellent creep properties owing to the optimal carbide characteristics at GBs.

ACKNOWLEDGMENTS

The authors thank Dr. J.Y. Wang and Mr. S.C. Yang for their help in mechanical property evaluation. The equipment support of processing from Mr. J.S. Chen, Dr. T.S. Lee, and Dr. Y.L. Lin is also thankfully acknowledged. The authors appreciate the financial support of this research by the National Science Council, Republic of China, under Grant No. NSC 86-2623-D-009-006.

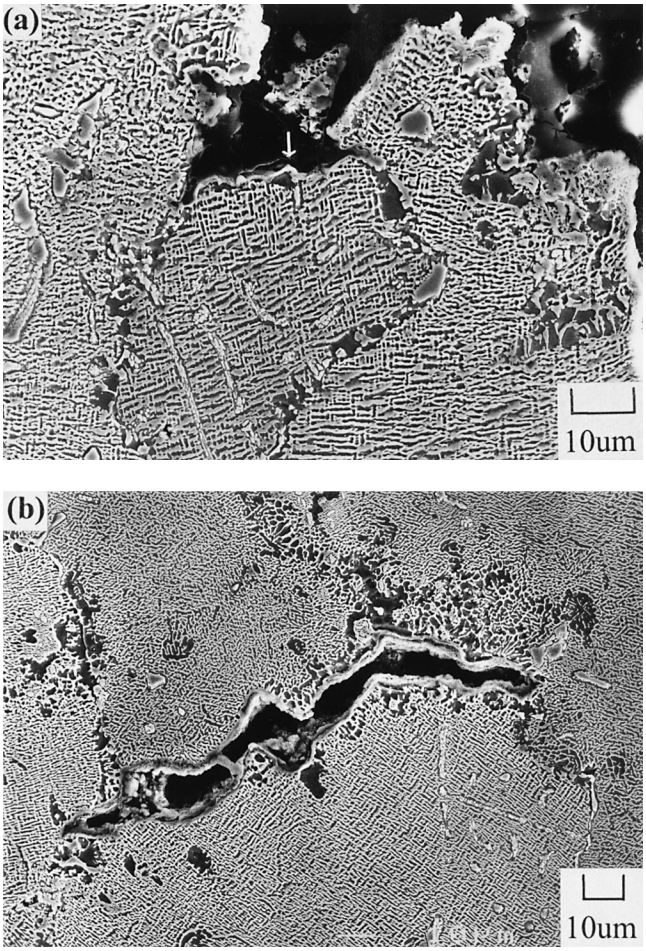

Fig. 10—Longitudinal section of a crept Mar-M247 superalloy containing 80 ppm Mg tested under 1255 K/200 MPa: (*a*) at the fracture position and (*b*) 100 μm from the fracture surface.

REFERENCES

1. J.E. Doherty, B.H. Kear, and A.F. Giamei: *J. Met.*, 1971, vol. 23(11), pp. 59-62.
2. D.N. Duhi and C.P. Sullivan: *J. Met.*, 1971, vo1. 23(7), pp. 38-40.
3. M.V. Nathal, R.D. Maier, and L.J. Ebert: *Metall. Trans. A*, 1982, vol. 13A, pp. 1767-74.
4. M.V. Nathal, R.D. Maier, and L.J. Ebert: *Metall. Trans. A*, 1982, vol. 13A, pp. 1775-83.
5. "Castings, Investment, MAR-M247," Allied-Signal Aerospace Company: Engine Materials Specification 55447, Allied-Signal Aerospace Company, Phoenix, AZ, 1988.
6. M. Kaufman: *Proc. Superalloys 1984*, M. Gell, C.S. Kortovich, R.H. Bricknell, W.B. Kent, and J.F. Radavich, eds., AIME, New York, NY, 1984, pp 43-52.
7. P.S. Kotval, J.D. Venables, and R.W. Calder: *Metall. Trans.*, 1972, vol. 3, pp. 453-58.
8. T.B. Gibbons and B.E. Hopkins: *J. Met. Sci.*, 1971, vol. 5, pp. 233-40.
9. H.Y. Bor, C.G. Chao, and C.Y. Ma: *Metall. Mater. Trans. A*, 1999, vol. 30A, pp. 551-61.
10. G.R. Leverant and M. Gell: *Trans. TMS-AIME*, 1969, vol. 245, pp. 1167-73.
11. J. Schramm: U.S. Patent No. 3512963, May 19, 1970.
12. L.M. Rober and N.C. Charlotte: U.S. Patent No. 4376650, March 15, 1983.
13. L.M. Rober and N.C. Charlotte: U.S. Patent No. 4456481, June 26, 1984.
14. J.M. Moyer: *Proc. Superalloys 1984*, M. Gell, C.S. Kortovich, R.H. Bricknell, W.B. Kent, and J.F. Radavich, eds., AIME, New York, NY, 1984, pp. 443-54.
15. P. Ma, Y. Yuan, and Z.Y. Zhong: *Proc. Superalloys 1988*, S. Reichman, D.N. Duhl, G. Maurer, S. Antolovich, and C. Lund, eds., AIME, New York, NY, 1988, pp. 625-33.
16. X.H. Xie, Z.H. Xu, B. Qu, and G.L. Chen: *Proc. Superalloys 1988*, S. Reichman, D.N. Duhl, G. Maurer, S. Antolovich, and C. Lund, eds., AIME, New York, NY, 1988, pp. 635-42.
17. Y.Q. Li, C.M. Sun, J.Y. Liu, and G.L. Chen: *High Temp. Technol.*, 1987, vol. 5(4), pp. 201-04.
18. G.L. Chen, T.H. Zhang, and W.Y. Yang: *High Temp. Technol.*, 1988, vol. 6(3), pp. 149-52.
19. Y.Q. Li and Y.H. Gong: *J. Mater. Sci.*, 1992, vol. 27, pp. 6641-45.
20. G.S. Chyernyak, A.V. Smirnova, and S.B. Maslenkov: *Metall. (Metalli.) SSSR*, 1973, No. 1 pp. 98-104.
21. V.V. Topilin: *Steel (Stal)*, 1978, No. 11 pp. 643-46.
22. X. Xie, K. Ni, Z. Xu, G. Ling, and N. Wang: *Mech. Behaviour Mater.*, 1991, vol. 4, pp. 613-18.
23. H.L. Ge, W.V. Youdelis, G.L. Chen, and Q. Zhu: *Mater. Sci. Technol.*, 1989, vol. 5, pp. 985-90.
24. G. Chen, Q. Zhu, D. Wang, and X. Xie: *in Superalloy 718*, E.A. Loria, ed., TMS, Warrendale, PA, 1989, pp. 545-51.
25. H.Y. Bor, C.G. Chao, and C.Y. Ma: *Scripta Mater.*, 1998, vol. 38(2), pp. 329-35.
26. P. Ma and J. Zhu: *Metallography*, 1986, vol. 19, pp. 115-18.
27. C.T. Sims: *J. Met.*, 1966, vol. 18, pp. 1119-30.
28. H.E. Gresham: *Met. Mater.*, 1969, vol. 3, p. 433.